

Molecular Motion Inside an Adsorbed [5:1] Fullerene Hexaadduct Observed by Ultrafast Cyclic Voltammetry**

Philippe Fortgang, Emmanuel Maisonhaute,* Christian Amatore,* Béatrice Delavaux-Nicot,* Julien Iehl, and Jean-François Nierengarten*

Charge injection at interfaces and charge transport through organic nanowires or nanoscale molecular assemblies play a key role in the development of nanoelectronic devices.^[1] On the other hand, charge hopping from one molecular electronic component to a neighboring one must be controlled and/or prevented at the molecular level to allow the design of electronic circuits from molecular components.^[2] A deeper understanding of all these processes is therefore very important. Among the possible techniques available to study them, ultrafast cyclic voltammetry (CV) is particularly appealing.^[3] Indeed, this method allows for the investigation of extremely fast molecular events that occur within nano- and sub-nanometer distances from a working-electrode surface. In other words, it is an extremely powerful tool for probing the efficiency of the electron transfer through an organic bridge that separates the electrode from the electroactive layer.^[4] On the other hand, this technique has been also used to demonstrate a multistep electron-hopping mechanism for the reduction and/or oxidation of redox centers attached to the periphery of dendritic systems adsorbed on the electrode surface.^[5] However, major drawbacks of the dendritic systems studied so far are the absence of spatial control on the redox centers because of the conformational flexibility of the dendritic scaffold^[6] and/or difficult reproducibility that results from the nonspecific adsorption of the molecules onto

the electrode surface.^[5,7] In order to gain a certain degree of control over the spatial organization in such multiple redox centers, they should be grafted onto a three-dimensional rigid scaffold, at the same time allowing specific anchoring onto the electrode surface.^[8] Indeed, the rigid spherical framework of hexasubstituted fullerene derivatives with a T_h -symmetrical octahedral addition pattern^[9] appears to be ideally suited for such a purpose. With this idea in mind, we prepared a mixed [5:1] fullerene hexaadduct that bears ten peripheral ferrocene redox subunits as well as 1,2-dithiolane moieties, thus allowing the anchoring onto a gold electrode. Ultrafast CV investigations of the resulting modified gold electrodes for the first time gave access to characteristic parameters for motion inside a macromolecule.

The synthesis of compound **5** relies on an approach recently reported by some of us for the efficient functionalization of mixed [5:1] fullerene hexaadducts.^[10] As shown in Scheme 1, the stepwise functionalization of the hexasubstituted fullerene scaffold is based on sequential copper(I)-catalyzed alkyne-azide cycloaddition reactions^[11] starting from building block **1**, thus allowing the successive grafting of two different peripheral groups. Reaction of **1** with ethynylferrocene (**2**) in the presence of $\text{CuSO}_4 \cdot 5\text{H}_2\text{O}$ and sodium ascorbate gave **3**. Subsequent treatment with azide **4** in the presence of tetrabutylammonium fluoride (TBAF), $\text{CuSO}_4 \cdot 5\text{H}_2\text{O}$, and sodium ascorbate in $\text{CH}_2\text{Cl}_2/\text{H}_2\text{O}$ gave the fully reacted [5:1] fullerene hexaadduct **5**. The ^{13}C NMR spectra of **3** and **5** reveal the strong influence of the high local symmetry (see Figure S1 in the Supporting Information). In each spectrum, two groups of signals appear for the fullerene sp^2 carbon atoms, which are reminiscent of those of the two nonequivalent fullerene sp^2 carbon atoms of the hexakis adduct that carries just one type of substituent (overall T_h symmetry). No influence of the overall C_{2v} symmetry of **3** and **5** can be deduced. Similar observations have been reported for other mixed hexaadducts of C_{60} .^[12] The expected signals of the unique malonate substituent are clearly distinguishable; the other five malonate substituents appear as pseudoequivalent and give rise to one set of signals similar to the one observed for the corresponding hexakis adducts that carry just one type of substituent. In the ^{13}C NMR spectrum of **3**, the typical signal of the sp^2 carbon atoms of the ten pseudoequivalent 1,2,3-triazole units^[10,13] are detected at $\delta = 119.2$ and 146.8 ppm (see Figure S1). The expected signals of the unique malonate substituent are also clearly distinguishable, thus showing that the TMS-protected alkyne units ($\text{TMS} = \text{trimethylsilyl}$) were not reactive under the conditions used for the preparation of **3**. The structure of **3** was further confirmed by its MALDI-TOF mass spectra that show the expected

[*] Dr. P. Fortgang, Prof. C. Amatore
UMR CNRS 8640 "PASTEUR", Ecole Normale Supérieure
Université Pierre et Marie Curie-Paris 06
24 rue Lhomond, 75231 Paris Cedex 05 (France)
E-mail: christian.amatore@ens.fr

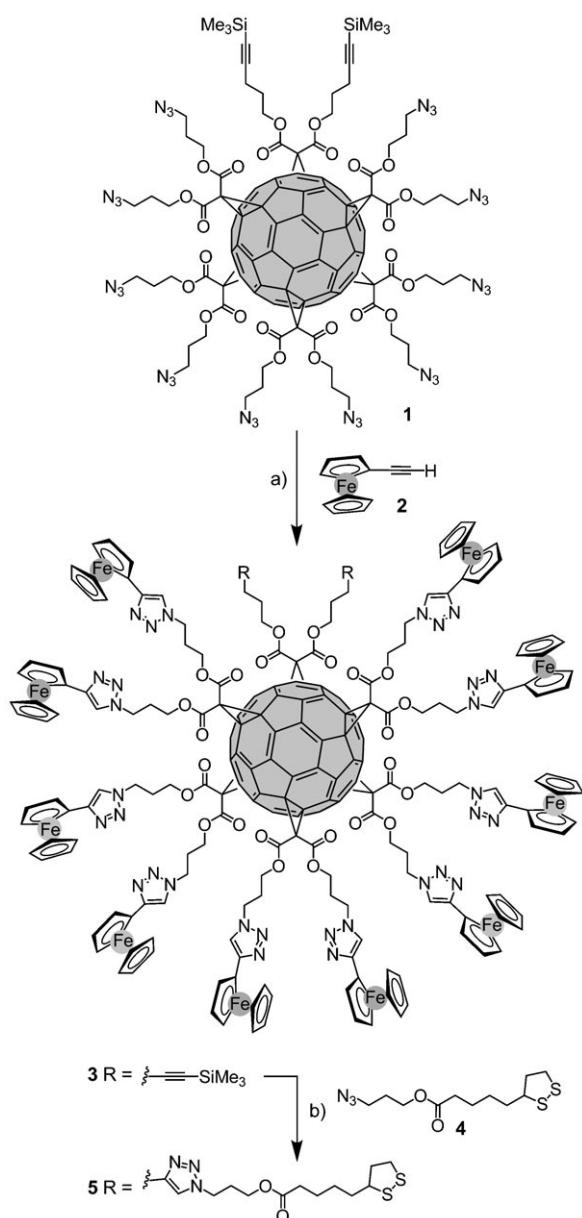
Prof. E. Maisonhaute
Laboratoire Interfaces et Systèmes Electrochimiques—UPR 15
Université Pierre et Marie Curie-Paris 06, 75005 Paris (France)
E-mail: emmanuel.maisonhaute@upmc.fr

Dr. B. Delavaux-Nicot
Laboratoire de Chimie de coordination du CNRS
Université de Toulouse (UPS, INP)
205 route de Narbonne, 31077 Toulouse Cedex 4 (France)
E-mail: beatrice.delavaux-nicot@lcc-toulouse.fr

Dr. J. Iehl, Prof. J.-F. Nierengarten
Laboratoire de Chimie des Matériaux Moléculaires
Université de Strasbourg et CNRS (UMR 7509)
Ecole Européenne de Chimie, Polymères et Matériaux
25 rue Becquerel, 67087 Strasbourg (France)
E-mail: nierengarten@chimie.u-strasbg.fr

[**] This work was supported by the CNRS (UMR 8640 and 7509, UPR 8241). J.I. thanks the University of Strasbourg for a fellowship. We further thank M. Schmitt for NMR measurements.

Supporting information for this article is available on the WWW under <http://dx.doi.org/10.1002/anie.201007289>.



Scheme 1. Reagents and conditions: a) sodium ascorbate, $\text{CuSO}_4 \cdot 5\text{H}_2\text{O}$, $\text{CH}_2\text{Cl}_2/\text{H}_2\text{O}$ 1:1, 25 °C (58%); b) TBAF, sodium ascorbate, $\text{CuSO}_4 \cdot 5\text{H}_2\text{O}$, $\text{CH}_2\text{Cl}_2/\text{H}_2\text{O}$ 1:1, 25 °C (70%).

molecular ion peak at m/z 4541 ($[M]^+$, calcd for $\text{C}_{244}\text{H}_{190}\text{Fe}_{10}\text{N}_{30}\text{O}_{24}\text{Si}_2$: 4541.02, Figure S2). Typical fragments that result from the loss of one or two ethynylferrocene moieties are also observed at m/z 4329 and m/z 4118, respectively. Retro-cycloaddition is a classical fragmentation pathway for 1,2,3-triazole derivatives^[14] but in the case of **3**, it prevented any definitive conclusions about the monodispersity of the isolated product. Conversely, IR data confirmed that no azide residues (2094 cm^{-1}) remain in the final product (Figure S3) and thus allowed us to conclude that no defected by-products are present. When going from **3** to **5**, inspection of the ^{13}C NMR spectra clearly indicates the disappearance of the TMS-protected alkyne unit. The two diagnostic resonan-

ces of the sp^2 carbon atoms of the newly formed triazole rings are also clearly observed in the ^{13}C NMR spectrum of **5**. IR data confirmed the absence of azide (2094 cm^{-1}) and alkyne (2172 cm^{-1}) residues in the final product (Figure S3). Finally, the structure of **5** was confirmed by its MALDI-TOF mass spectrum, which shows the expected molecular ion peak at m/z 4975.1 ($[M]^+$, calculated for $\text{C}_{260}\text{H}_{212}\text{Fe}_{10}\text{N}_{36}\text{O}_{28}\text{S}_4$: 4975.48, Figure S4).

After a general electrochemical study of **5** (see the Supporting Information), we focused on the first oxidation wave, which is related to oxidation of the ferrocene entities. Compound **5** was adsorbed onto a gold ultramicroelectrode to form a submonolayer and probe the dynamic exchange of electrons inside isolated molecules. Voltammograms obtained upon varying the scan rate ν over a large range for a $7\text{ }\mu\text{m}$ wide and 3.2 mm long modified electrode^[15] are depicted in Figure 1. At slow scan rates, well-defined bell-shape curves are obtained, as expected for adsorbed material.^[16] The peak

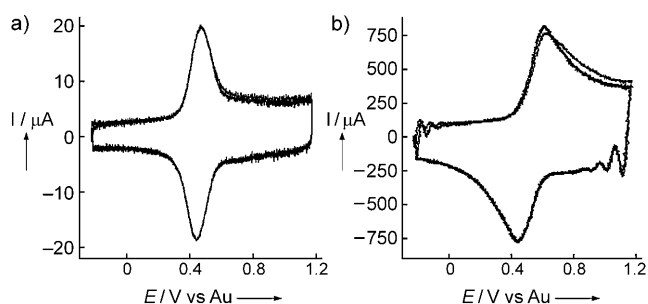


Figure 1. Voltammograms of compound **5** adsorbed onto a gold ultramicroelectrode (three consecutive scans) in CH_3CN + 1 M tetra-*n*-butylammonium tetrafluoroborate at a) 836 Vs^{-1} and b) 55700 Vs^{-1} .

half width is nevertheless higher than the expected 90.6 mV for an ideal Nernstian behavior as often observed with such systems. Slightly different environments for redox centers and interactions between them can be invoked to explain this nonideal behavior. In the slow ν regime, the peak intensity scales directly with ν , the slope being proportional to the number of adsorbed molecules (Figure 1a). A surface coverage of $1.0 \times 10^{-7}\text{ mol m}^{-2}$ can thus be estimated. This number is slightly smaller than the one obtained by charge integration ($1.5 \times 10^{-7}\text{ mol m}^{-2}$) as a consequence of the slightly nonideal behavior of the voltammogram.

Upon increasing the scan rate (Figure 1b), the peak potentials shift a little because the voltametric rate ($F\nu/RT$) compares to the one related to electron transfer between the electrode and the redox sites in its proximity. More importantly, the waves broaden, thus giving a first indication that conversely to the slow regime only a fraction of the ferrocene subunits of **5** are oxidized during the forward scan.^[3,5-7] Indeed, at low scan rates, ferrocene entities that lie too far from the surface cannot communicate directly with the electrode since the electronic coupling is too weak. These ferrocene moieties can however be oxidized in a multistep

hopping mechanism that involves neighboring ferricinium entities according to Equation (1):



Figure 2 shows the peak current divided by $v^{1/2}$ versus $v^{1/2}$ for **5**. Typically, previously investigated electroactive dendrimers similarly displayed a plateau at high scan rates owing

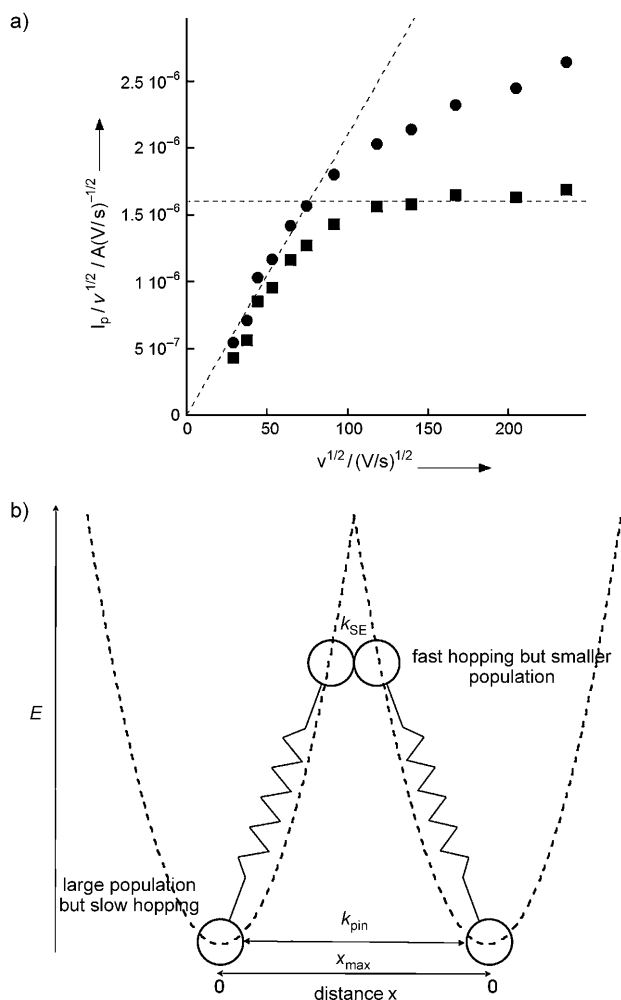


Figure 2. a) Peak potential dependence on the scan rate (spheres: experimental data; squares: a slope of 4×10^{-9} A has been subtracted from the experimental data). b) Schematic representation of the movement of redox centers in a harmonic potential well to facilitate electron hopping.

to the fact that the oxidation wave cannot propagate through the whole molecule when the timescale is shortened as observed for other systems.^[5,7] The situation then becomes similar to diffusion of redox species in solution, albeit here it concerns diffusion of electrons over a molecular truncated sphere. We have previously examined this situation in detail for a polyamidoamine dendrimer modified by 64 $[\text{Ru}(\text{tpy})_2]^{2+}$ redox centers (tpy = terpyridine).^[5] We demonstrated that the plateau value depends on the quantity $D_{\text{hop}}^{1/2} \tan(\phi_0/2)/r$, where ϕ_0 is the half angle of the truncated sphere, r the

macromolecule radius ($1.3 < r < 1.55$ nm as estimated by molecular simulations), and D_{hop} the apparent diffusion coefficient that is proportional to the rate of the homogeneous exchange reaction k_{hop} [Eq. (2)].

$$D_{\text{hop}} = \frac{2k_{\text{hop}}}{3\pi d N_A} \quad (2)$$

where d is the diameter of a ferrocene redox center (anticipated as a sphere), and N_A is the Avogadro number.

In the case of **5**, the slope diminishes but a plateau is however not reached (Figure 2a). Our interpretation is that some redox centers nearby the electrode remain independent so that their contribution is still proportional to v (pure adsorption behavior, no electron hopping, at least for fast v). A second population results from redox centers that interact with one another, thus giving a contribution proportional to v in the long-timescale regime (small v) and to $v^{1/2}$ in the short timescale regime (fast v), as was formerly observed. The experimental voltammogram would then simultaneously feature the contributions of these two populations. This assumption is corroborated by the observation that a plateau behavior is recovered when more compact monolayers or multilayers are formed; it is likely that in this case there are no isolated entities. Accurately estimating both contributions from the sole analysis of the peak currents is accompanied by several difficulties. A first problem is that peak shape and the maximum positions differ for the two populations, particularly in the short timescale regime. However, we estimated that it would result in a maximum error of 20% so that the break in the slope observed in Figure 2a reflects a true physical phenomenon and is not an artifact (see the Supporting Information).

To perform a semiquantitative analysis, we subtracted a slope of 4×10^{-9} A from the experimental data, in order to obtain a curve that now displays a plateau at $1.6 \times 10^{-6} \text{ A s}^{1/2} \text{ V}^{-1/2}$ (squares in Figure 2a). The slope ratio between the two curves in the low scan rates regime suggests that two redox centers out of ten act independently. If the ferrocene entities were displayed regularly at the apexes of an icosahedron, ϕ_0 could be expected to be around 60° . Removing the two most proximal sites leads to $\phi_0 \approx 90^\circ$. Considering these experimental uncertainties, we estimated that D_{hop} spans the range of 1.9×10^{-9} to $1.3 \times 10^{-8} \text{ cm}^2 \text{ s}^{-1}$ for $60 < \phi_0 < 90^\circ$ and $1.3 < r < 1.55$ nm, thus leading to k_{hop} between $3.3 \times 10^5 \text{ L mol}^{-1} \text{ s}^{-1}$ and $2.2 \times 10^6 \text{ L mol}^{-1} \text{ s}^{-1}$, anticipating a diameter $d = 0.614$ nm for the ferrocene.

For independent ferricinium and ferrocene in contact in acetonitrile, self-exchange rates have been measured by several methods. Initially, NMR spectroscopy line broadening was used, and a value of $k_{\text{SE}} = 7.5 \times 10^6 \text{ L mol}^{-1} \text{ s}^{-1}$ was estimated,^[17] which was confirmed by the stopped flow technique ($7.1 \times 10^6 \text{ s}^{-1}$).^[18] Remarkably, the nature and the concentration of the supporting electrolyte play only a minor role. Our values are much smaller compared to the situation in which the redox centers are touching each other. Indeed, it is well known that electron-transfer efficiency diminishes exponentially with the distance with an estimated attenuation factor λ between 10 and 20 nm^{-1} .^[19] We thus subsequently

take 10 nm^{-1} for λ as a minimum value. A distance between 0.376 and 0.508 nm can be estimated between the edges of the ferrocene entities shown at the apexes of an icosahedron. If the redox centers were pinned at these positions, rates in the range $2.9 \times 10^2 < k_{\text{pin}} < 4.0 \times 10^3 \text{ L mol}^{-1} \text{ s}^{-1}$ can be estimated, a value much smaller than the ones we deduce. The experimental intermediate situation is resolved by considering that molecular motions favor electron transfer, but that the linking chains retain the electroactive entities so that $k_{\text{pin}} \leq k_{\text{hop}} \leq k_{\text{SE}}$ as sketched in Figure 2b. Our former analysis considered a viscous motion in a harmonic potential well.^[5b] Two limiting cases were highlighted; in the first one, viscosity is negligible, and the redox center population is given by a Boltzmann relationship. In the second one, viscous friction in the potential well hampers reaching the equilibrium. Experimentally, we cannot discriminate between these two situations; nevertheless, in this molecule the linking chains are not close so that we expect no important viscous damping. Consequently, we rely on the harmonic limitation to pursue the interpretation and considering the most efficient antisymmetric movement of the redox centers along the x reaction coordinate gives an expression for k_{hop} [Eq. (3) and Figure 2b]:

$$k_{\text{hop}}(x) = k_{\text{pin}} \exp(2\lambda x) \exp\left(-\frac{\kappa x^2}{k_{\text{B}} T}\right) \quad (3)$$

where κ is the stiffness constant of the harmonic spring. In Equation (3) the first exponential term stems from the distance dependence of electronic coupling, while the second one takes into account the diminished probability of finding a redox entity away from its equilibrium position. k_{hop} is optimal either for $x = x_{\text{opt}} = \lambda k_{\text{B}} T / \kappa$ if $(\lambda k_{\text{B}} T / \kappa) < x_{\text{max}}$, the distance of the closest approach, or for $x = x_{\text{max}}$ if $(\lambda k_{\text{B}} T / \kappa) > x_{\text{max}}$. In our case, we find that whatever the hypothesis, electron transfer occurs at contact and we can thus estimate κ to range between $1.9 \times 10^{-2} < \kappa < 9.1 \times 10^{-2} \text{ J m}^{-2}$. Taking larger λ values would lead to even smaller stiffness; we therefore deduce that rather large movements are possible on the dendrimer shell.

This original example of electronic molecular communication reveals that even for a limited number of redox sites, a diffusive model still provides very useful insights. The deduced parameters allow a simple characterization of the structure deformation and flexibility inside a single molecule.

Received: November 19, 2010

Published online: February 11, 2011

Keywords: cycloaddition · electrochemistry · ferrocenes · fullerenes · ultrafast cyclic voltammetry

- M. R. Wasielewski, *Angew. Chem.* **2010**, *122*, 2966–2970; *Angew. Chem. Int. Ed.* **2010**, *49*, 2904–2908, and references therein; c) D. M. Guldi, *Angew. Chem.* **2010**, *122*, 8016–8018; *Angew. Chem. Int. Ed.* **2010**, *49*, 7844–7846.
- [2] J. Jortner, M. Ratner, *Molecular Electronics*, Blackwell, London, **1997**.
- [3] C. Amatore, E. Maisonhaute, J.-F. Nierengarten, B. Schöllhorn, *Isr. J. Chem.* **2008**, *48*, 203–214.
- [4] C. E. D. Chidsey, *Science* **1991**, *251*, 919–922; C. Amatore, E. Maisonhaute, B. Schöllhorn, J. Wadhawan, *ChemPhysChem* **2007**, *8*, 1321–1329.
- [5] a) C. Amatore, Y. Bouret, E. Maisonhaute, J. I. Goldsmith, H. D. Abruña, *ChemPhysChem* **2001**, *2*, 130–134; b) C. Amatore, Y. Bouret, E. Maisonhaute, J. I. Goldsmith, H. D. Abruña, *Chem. Eur. J.* **2001**, *7*, 2206–2226; c) C. Amatore, E. Maisonhaute, *Anal. Chem.* **2005**, *77*, 303A–311A.
- [6] J. A. Camerano, M. A. Casado, U. Hahn, J.-F. Nierengarten, E. Maisonhaute, C. Amatore, *New J. Chem.* **2007**, *31*, 1395–1399.
- [7] U. Hahn, E. Maisonhaute, C. Amatore, J.-F. Nierengarten, *Angew. Chem.* **2007**, *119*, 969–972; *Angew. Chem. Int. Ed.* **2007**, *46*, 951–954.
- [8] A. F. Wang, C. Ornelas, D. Astruc, P. Hapiot, *J. Am. Chem. Soc.* **2009**, *131*, 6652.
- [9] For a review on fullerene hexakis adducts, see: A. Hirsch, O. Vostrowsky, *Eur. J. Org. Chem.* **2001**, 829–848.
- [10] J. Iehl, J.-F. Nierengarten, *Chem. Eur. J.* **2009**, *15*, 7306–7309.
- [11] a) R. Huisgen, *Pure Appl. Chem.* **1989**, *61*, 613–628; b) C. W. Tornøe, M. Meldal, *Proceedings of the 2nd International and 17th American Peptide Symposium, Peptides: The Waves of the Future*, (Eds.: M. Lebl, R. A. Houghton), San Diego, **2001**, pp. 263–264; c) V. V. Rostovtsev, L. G. Green, V. V. Fokin, K. B. Sharpless, *Angew. Chem.* **2002**, *114*, 2708–2711; *Angew. Chem. Int. Ed.* **2002**, *41*, 2596–2599.
- [12] a) A. Herzog, A. Hirsch, O. Vostrowsky, *Eur. J. Org. Chem.* **2000**, 171–180; b) J. Iehl, J.-F. Nierengarten, *Chem. Commun.* **2010**, 46, 4160–4162.
- [13] J. Iehl, R. Pereira de Freitas, B. Delavaux-Nicot, J.-F. Nierengarten, *Chem. Commun.* **2008**, 2450–2452.
- [14] a) M. A. Fazio, O. P. Lee, D. I. Schuster, *Org. Lett.* **2008**, *10*, 4979–4982; b) J. Iehl, M. Holler, J.-F. Nierengarten, K. Yoosaf, J. M. Malicka, N. Armaroli, J.-M. Strub, A. Van Dorsselaer, B. Delavaux-Nicot, *Aust. J. Chem.* **2010**, DOI: 10.1071/CH10319.
- [15] P. Fortgang, C. Amatore, E. Maisonhaute, B. Schöllhorn, *Electrochem. Commun.* **2010**, *12*, 897–900.
- [16] A. J. Bard, L. R. Faulkner, *Electrochemical Methods*, Wiley, New York, **2001**.
- [17] a) E. S. Yang, M. S. Chan, A. C. Wahl, *J. Phys. Chem.* **1980**, *84*, 3094; b) T. Gennett, M. J. Weaver, *J. Electroanal. Chem.* **1985**, *186*, 179; c) R. M. Nielson, G. E. McManis, L. K. Safford, M. J. Weaver, *J. Phys. Chem.* **1989**, *93*, 2152.
- [18] a) S. F. Nelsen, M. T. Ramm, R. F. Ismagilov, M. A. Nagy, D. A. Trieber, D. R. Powell, X. Chen, J. J. Gengler, Q. L. Qu, J. L. Brandt, J. R. Pladziewicz, *J. Am. Chem. Soc.* **1997**, *119*, 5900–5907; b) S. F. Nelsen, R. F. Ismagilov, K. E. Gentile, M. A. Nagy, H. Q. Tran, Q. L. Qu, D. T. Halfen, A. L. Odegard, J. R. Pladziewicz, *J. Am. Chem. Soc.* **1998**, *120*, 8230–8240; c) A. Zahl, R. van Eldik, M. Matsumoto, T. W. Swaddle, *Inorg. Chem.* **2003**, *42*, 3718–3722.
- [19] J. F. Smalley, M. D. Newton, S. W. Feldberg, *J. Electroanal. Chem.* **2006**, *589*, 1–6.

[1] a) *Electron Transfer in Chemistry* (Ed.: V. Balzani), Wiley, Weinheim, **2001**; b) A. M. Scott, A. Butler Ricks, M. T. Colvin,